

Kazrin, and Its Binding Partners ARVCF- and Delta-Catenin, Are Required for *Xenopus laevis* Craniofacial Development

Kyucheol Cho,^{1,2†} Moonsup Lee,^{1,2†} Dongmin Gu,^{1,2} William A. Munoz,^{1,2} Hong Ji,¹ Malgorzata Kloc,³ and Pierre D. McCrea^{1,2*}

The novel adaptor protein Kazrin associates with multifunctional entities including p120-subfamily members (ARVCF-, delta-, and p0071-catenin). Critical contributions of Kazrin to development or homeostasis are indicated with respect to ectoderm formation, integrity and keratinocyte differentiation, whereas its presence in varied tissues suggests broader roles. We find that Kazrin is maternally loaded, is expressed across development and becomes enriched in the forming head. Kazrin's potential contributions to craniofacial development were probed by means of knockdown in the prospective anterior neural region. Cartilaginous head structures as well as eyes on injected sides were reduced in size, with molecular markers suggesting an impact upon neural crest cell establishment and migration. Similar effects followed the depletion of ARVCF (or delta-catenin), with Kazrin:ARVCF functional interplay supported upon ARVCF partial rescue of Kazrin knockdown phenotypes. Thus, Kazrin and its associating ARVCF- and delta-catenins, are required to form craniofacial tissues originating from cranial neural crest and precordial plate. *Developmental Dynamics* 240:2601–2612, 2011. © 2011 Wiley Periodicals, Inc.

Key words: Kazrin; ARVCF-catenin; delta-catenin; craniofacial development

Accepted 1 August 2011

INTRODUCTION

Kazrin was first cloned as an uncharacterized human brain gene product, and then shown to be present at the mRNA level in other human tissues (Kikuno et al., 1999; Groot et al., 2004). The human *Kazrin* gene is located on chromosome 1p36.21, producing a transcript that is alternatively spliced to generate at least seven isoforms (A–F and K) (Groot

et al., 2004; Nachat et al., 2009; Wang et al., 2009; Cho et al., 2010). Various functions have been proposed for Kazrin, with some already tied to particular isoform interactions or localizations. An early study found that exogenous Kazrin expression inhibits clathrin-mediated internalization of the transferrin receptor, suggesting endocytic roles (Schmelzl and Geli, 2002). Research in human keratinocytes then pointed to several contribu-

tions, such as in structuring of the cornified envelope of skin (ectoderm barrier function), as a modulator of RhoA (cytoskeletal and additional functions), and in keratinocyte differentiation (Groot et al., 2004; Sevilla et al., 2008a). In U373MG human astrocytoma cells, Kazrin depletion correlated with caspase activation and apoptosis (Wang et al., 2009). In animal models, *Xenopus tropicalis* Kazrin was implicated in ectoderm

Additional Supporting Information may be found in the online version of this article.

¹Department of Biochemistry and Molecular Biology, The University of Texas M.D. Anderson Cancer Center, Houston, Texas

²Program in Genes & Development, University of Texas Graduate School of Biomedical Science – Houston, Houston, Texas

³Immuno-biology Laboratory, The Methodist Hospital Research Institute, The Methodist Hospital, Houston, Texas

Grant sponsor: National Institutes of Health; Grant number: RO1-GM52112; Grant sponsor: University of Texas MD Anderson Cancer Center; Grant number: NCI Core Grant CA-16672.

[†]Dr. Cho and M.S. Lee contributed equally to this work.

*Correspondence to: Pierre D. McCrea, Department of Biochemistry and Molecular Biology, The University of Texas M. D. Anderson Cancer Center, 1515 Holcombe Boulevard, Houston, TX 77030. E-mail: pdmccrea@mdanderson.org

DOI 10.1002/dvdy.22721

Published online 25 October 2011 in Wiley Online Library (wileyonlinelibrary.com).

integrity, eye formation and axial elongation (Sevilla et al., 2008b). Recently, in the closely related species, *Xenopus laevis*, we reported that Kazrin binds ARVCF-catenin (Armadillo Repeated gene deleted in VeloCardio Facial syndrome), as well as to two other p120-subfamily members, delta- and p0071-catenin (intriguingly not p120 itself) (Cho et al., 2010). We found that Kazrin works together with ARVCF in small-GTPase modulation through their mutual interaction with p190B-RhoGAP, potentially accounting for observed effects upon cadherin levels and cell-cell interactions. We further determined that Kazrin binds Spectrin, best known for its cytoskeletal and junctional roles (Bennett and Healy, 2009).

The vertebrate p120-catenin subfamily shares several features with those of the beta-catenin subfamily (beta-catenin and gamma-catenin/plakoglobin) (McCrea and Gu, 2010). For example, a central Armadillo domain is used by each catenin in binding cadherin cytoplasmic tails (Huber et al., 1997). Of interest, whereas 120-subfamily members bind proximal to the plasma membrane, beta-catenin subfamily members bind distal, with binding competition occurring within but not across subfamilies (Yap et al., 1998; Ohkubo and Ozawa, 1999; Mariner et al., 2000; Thoreson et al., 2000). When bound, p120-, ARVCF- or delta-catenin enhances the stability of classical cadherins through the reduction of cadherin endocytosis (Ireton et al., 2002; Davis et al., 2003; Xiao et al., 2003, 2005; Fang et al., 2004; Gu et al., 2009). Intriguingly, when not directly bound to cadherins, p120-subfamily members more potently associate with and regulate small-GTPases, having an impact upon cytoskeletal control and likely other intracellular signaling events (Anastasiadis et al., 2000; Noren et al., 2000; Grosheva et al., 2001; Anastasiadis, 2007). For example, in *Xenopus*, we find that the depletion of any p120-subfamily member measurably reduces cadherin levels and alters Rho-GTPase functions (Fang et al., 2004; Gu et al., 2009). Depletions result in gastrulation failures and effects that are partially or largely rescued upon

carefully titrated expression of the depleted catenin, or of a closely related subfamily member. With an independent study likewise reporting p120's roles in *Xenopus* craniofacial and eye development (Ciesiolka et al., 2004), it appears that each subfamily member is involved in multiple developmental processes. For reasons that likely include cross-species differences in delta-catenin's spatial or quantitative expression, the amphibian knock-down phenotypes for delta-catenin or ARVCF (Fang et al., 2004; Gu et al., 2009), have proven more dramatic than the corresponding knock-outs in mice (Israely et al., 2004; Davis and Reynolds, 2006). Of better correspondence is the knock-down/knock-out of p120 itself, which is early embryonic lethal regardless of the vertebrate system (Fang et al., 2004; Davis and Reynolds, 2006), with p0071 still to be examined/compared.

Returning to consideration of Kazrin as a binding partner of certain p120-subfamily members (all but p120 itself), it should be noted that the depletion of Kazrin in *Xenopus* embryos does not phenocopy depletion of ARVCF- or delta-catenin (Cho et al., 2010). This may be partially due to the existence of large maternal stores of Kazrin protein, such that the injection of anti-Kazrin morpholino oligonucleotides at the two- or four-cell stage does not result in Kazrin depletion until late (post gastrula) developmental stages. Functional interactions are indeed indicated, however, in that ectodermal disruption phenotypes following Kazrin knock-down are partially rescued by means of titrated exogenous expression of ARVCF-catenin (Cho et al., 2010).

We report here the consequences of Kazrin depletion in the forming vertebrate head region, where Kazrin is normally enriched. We find that Kazrin is essential for *Xenopus* craniofacial and eye development, with Kazrin depletion producing effects similar to knock-down of ARVCF- or delta-catenin, and Kazrin knock-down being partially rescued upon the expression of ARVCF. Our study points to Kazrin's requirement in later developmental events, and provides further evidence of its functional relationship with members of the p120-catenin subfamily.

RESULTS

Expression of Kazrin in *Xenopus laevis*

To obtain a preliminary indication of where Kazrin may function, we assessed the developmental spatiotemporal expression pattern of Kazrin mRNA using whole-mount in situ hybridization (Fig. 1A–E). In accordance with previous results from *Xenopus tropicalis* (Sevilla et al., 2008b), *Xenopus laevis* Kazrin transcripts were enriched in the ectodermal region at the late gastrulation stage (Fig. 1A); in the dorsal neural fold and anterior region at neurula stages (Fig. 1B); and in the head and eye at tail bud stages (Fig. 1C). Transverse sections of tadpoles revealed specific expression of Kazrin mRNA in the neural tube and eye (Fig. 1D). In addition, tadpole embryos subject to more prolonged in situ color reactions showed to quite variable but reproducible extents the expression of Kazrin in the dorsal part of the trunk and overall head area, with characteristic pharyngeal arch staining (arrowhead in enlarged image of Fig. 1E).

Constitutive expression of Kazrin transcripts throughout early development were detected by conducting semi-quantitative reverse transcriptase-polymerase chain reaction (RT-PCR) assay (Supp. Fig. S1, which is available online). Our earlier study revealed the existence of two Kazrin isoforms in *Xenopus laevis*. It is notable that, while xKazrinB transcripts were detected from the one-cell embryo through tadpole stages, xKazrinA transcripts were only resolved during or after gastrulation (stage 12).

To evaluate the temporal expression of xKazrin at the protein level, embryonic lysates were prepared from various developmental stages and subjected to immuno-blotting using an IgG-purified polyclonal antibody raised against the carboxyl terminal 147 amino acids of xKazrinA. In common with mammals, *Xenopus* embryos express two major Kazrin protein bands migrating at approximately 40 kDa and 47 kDa, respectively (Fig. 1F). Both proteins appeared to be constitutively expressed from the oocyte through tadpole stages. The *Xenopus* 40 kDa band corresponds to the size of

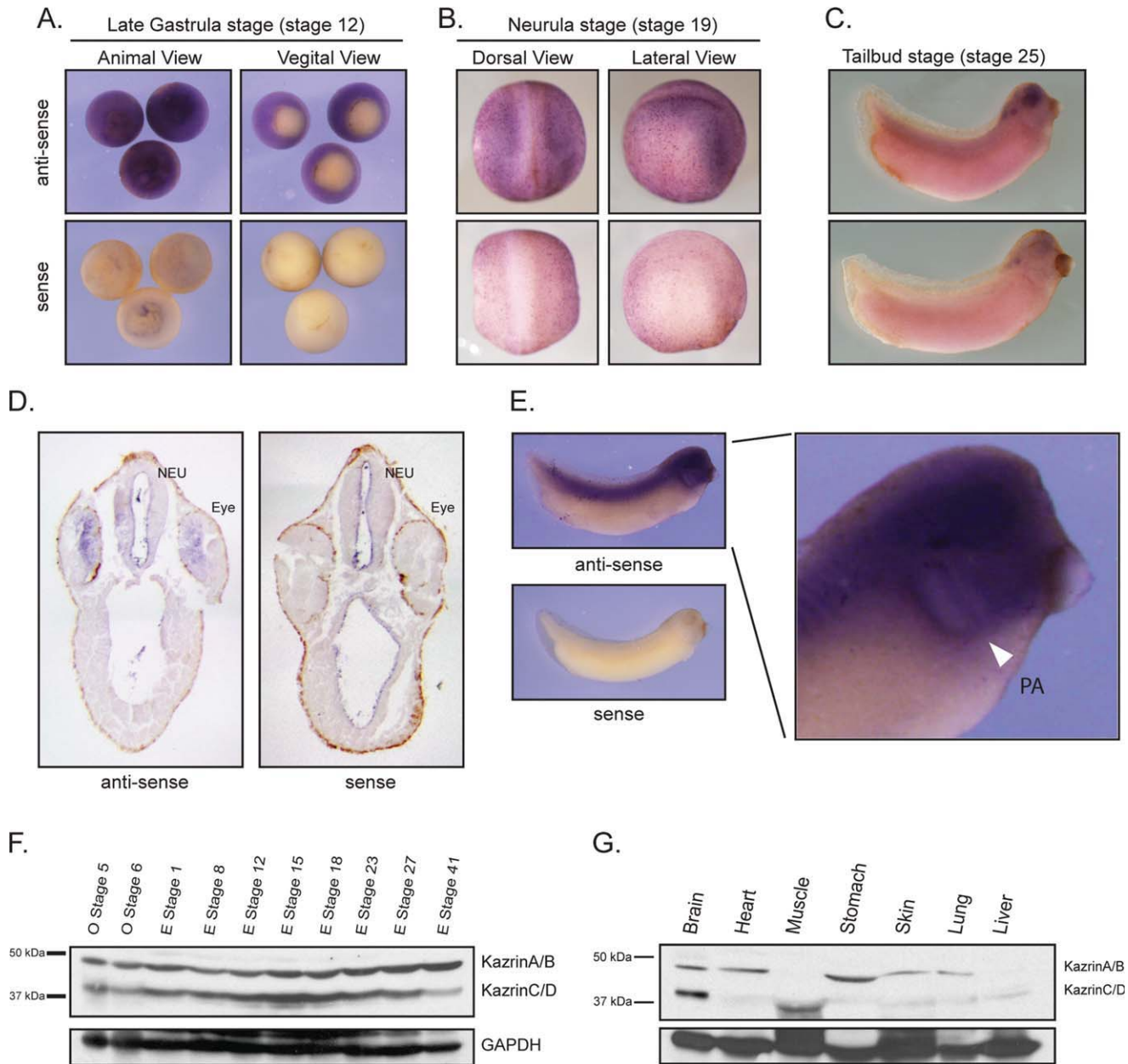


Fig. 1. xKazrin expression during *Xenopus* development. **A–C:** xKazrin spatio-temporal expression was assessed by means of in situ hybridization of late gastrula (A), neurula (B), and tadpole stage embryos (C). The probe consisted of Dig-labeled anti-sense RNA of full-length xKazrinA, while the negative control was the sense counterpart. **D:** Kazrin mRNA expression in the head region of tadpoles shown in (C) were visualized using microtome sectioning. Brain neural tube (NEU) and eye (Eye) are indicated. **E:** Extensive Kazrin mRNA signal was obtained upon prolonged substrate reaction. Right panel shows enlarged image of the head region. Pharyngeal arch (PA) is indicated by an arrowhead. **F:** *Xenopus* embryo lysates taken from varying stages as indicated (0.5 embryo/ lane) were subject to SDS-PAGE and immuno-blotted for xKazrin (polyclonal antibody directed against carboxyl 147 amino acids of xKazrinA and IgG purified), or for GAPDH (glyceraldehyde-3-phosphate dehydrogenase; loading control (bottom panel)). **G:** Immuno-blot of *Xenopus* adult tissues (SDS-soluble fraction) as indicated. xKazrin was detected as 47 kDa (KazrinA or B) and 40 kDa (KazrinC/D) isoforms. Equal total protein was loaded per lane, and actin used as a loading control. Molecular weights are indicated in kilodaltons (kDa).

the human Kazrin C/D isoform, consistent with the possible existence of this or a similar isoform in *Xenopus*. The predicted molecular weight of xKazrinA is 46.8 kDa, and exogenously expressed xKazrinA migrates at ~47 kDa (data not shown), suggesting that the isoform detected at ~47 kDa may

be KazrinA. However, because xKazrinA mRNA was not detected until the blastula stage by means of RT-PCR (Supp. Fig. S1), the ~47 kDa band may instead be xKazrinB. It is notable that previous studies showed injection of a translation blocking morpholino (Kmo-1) decreased expression of this band

(Sevilla et al., 2008b; Cho et al., 2010). Brain, heart, stomach, skin and lung exhibit a protein migrating at 47 kDa (likely xKazrinA or B) (Fig. 1G). Brain expresses an additional 40 kDa xKazrin (possibly xKazrinC/D), with even lesser amounts of the 40 kDa xKazrin isoform appearing in other tissues. In

all cases, across both developmental stages (time) and tissues (space), xKazrin protein and transcript isoforms show variable expression.

Assessment of xKazrin Morpholinos

We and another group earlier reported in *Xenopus tropicalis* and *laevis* that depletion of Kazrin using a translation-blocking morpholino results in ectodermal blistering and other phenotypes (Sevilla et al., 2008b; Cho et al., 2010). For the present study, we designed another Kazrin morpholino (Kmo-S), that blocks nuclear processing of xKazrin pre-mRNA. Kazrin Mo-S was designed to bind the 3' end of exon 4 (Fig. 2A), inhibiting its proper splicing. As expected, RT-PCR analysis following morpholino injection revealed that the diagnostic product decreased in a dose-dependent manner, consistent with exon 4 skipping (Fig. 2B, F1/R1 PCR product). This was confirmed upon DNA sequencing of the lower F1/R2 product band (data not shown). Of interest, the F1/R2 primer-pair product was not observed upon high-dose morpholino injection (Fig. 2B, right lane), consistent with exon 4 skipping producing a frame-shift in exon 5 followed by a nonsense mutation, and thus initiation of nonsense-mediated decay (NMD) (Singh and Lykke-Andersen, 2003).

We next evaluated phenotypes arising in embryos after Kazrin Mo-S injection. Unlike embryos subjected to the standard-control morpholino (SCmo), those injected with Kmo-S exhibited severe ectoderm and neur ectoderm defects leading to abnormal neural tube closure (Fig. 2C,a'b'), and to regional ectoderm shedding during neurulation (Fig. 2C,c'). The fraction of embryos exhibiting such phenotypes increased with increasing morpholino dose (Supp. Fig. S2).

To assay for changes in inner tissue structures, hematoxylin stained sections of Kmo-S injected embryos were analyzed by light microscopy. Small and ill-formed neural tubes, in addition to displaced adjoining myotomal tissues were readily apparent (Fig. 2D). As seen earlier from external viewings, the integrity of the dorsal epithelium was often compromised, exposing inner cells that appeared

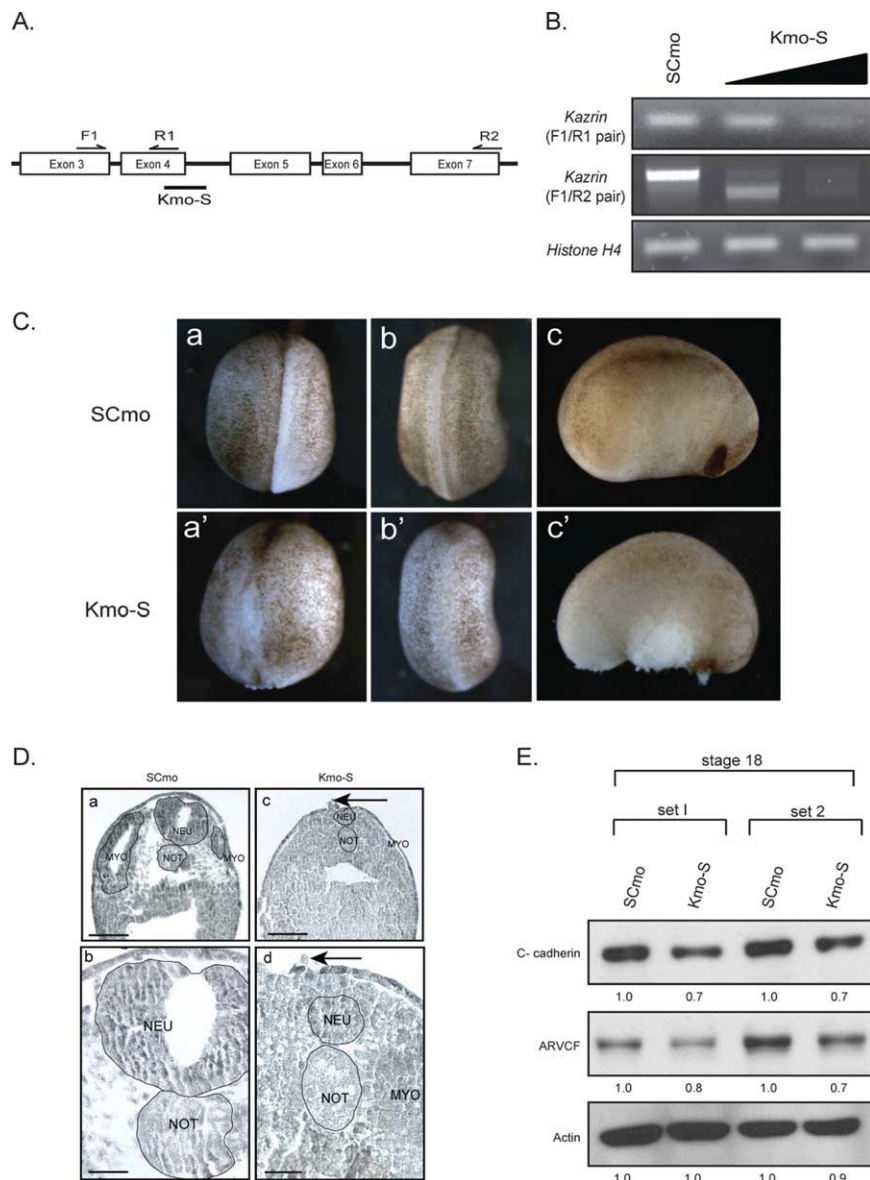


Fig. 2. Assessment of xKazrin morpholino-S (Kmo-S). **A:** Schematic diagram of morpholino binding region and primers used for testing morpholino effectiveness (left panel). **B:** Impact of Kmo-S on expression of endogenous xKazrin RNA, assayed using reverse transcriptase-polymerase chain reaction (RT-PCR). Embryos were injected with two doses of Kmo-S (40 ng or 80 ng), total RNA was isolated from stage 18–19 embryos, and RT-PCR conducted using the indicated primer pairs. Standard Control morpholino (SCmo) was used as a negative control. **C:** Reduced ectoderm integrity results following Kmo-S injection. Stage 20–22 embryos are shown following Kmo-S (a', b', and c') versus SCmo (a, b, and c) injections into the animal region of 1-cell stage embryos or into both cells of 2-cell stage embryos. 80 ng of morpholino total was injected into each embryo. **D:** Hematoxylin stained sections of SCmo injected (a & b) versus Kmo-S morpholino injected (c & d) stage 20 embryos. Depletion of xKazrinA resulted in altered structure and organization of the neural tube (NEU), notochord (NOT), and myotome (MYO). Morpholino injected embryos in many instances displayed the sloughing of ectodermal cells (arrows) on the dorsal side (Fig. 2Ca'), or elsewhere (Fig. 2Cc'). Scale bar = 300 μ m in a,c; 80 μ m in b,d. What appears to be asymmetrical myotome structure in Figure 2Da is in fact due to nonperpendicular sectioning. **E:** Decrease of cadherin and ARVCF-catenin protein levels after xKazrin depletion using Kmo-S morpholino. Embryos injected at the one-cell stage with different amounts of the indicated morpholinos were lysed at early gastrula (stage 10) stage. Indicated protein levels were visualized by immuno-blotting, and normalized band intensities were obtained using the software analysis program Image J.

to be in the process of dissociating from the embryo body (arrows in Fig. 2D,c,d).

Our prior study showed that Kazrin depletion using a translation blocking morpholino resulted in decreased

cadherin and catenin levels. Kmo-S injection had the same impact (Fig. 2E), suggesting that Kmo-S is functionally comparable to the Kazrin translation blocking morpholino.

xKazrin Depletion in the Head Region Induces Eye and Craniofacial Defects

Whole-mount in situ hybridization revealed that *Kazrin* mRNA is expressed in the head region of neurula and tail bud embryos (Fig. 1B,C,E), and Kazrin protein isoforms are detected in adult brain tissue (Fig. 1G). Together with its initial cloning from a mouse brain cDNA library (Kikuno et al., 1999), these results suggested that Kazrin may function in head or brain formation. To address this possibility, xKazrin was specifically depleted in the future head region by injecting xKazrin morpholinos (Kmo-1 or Kmo-S) into the animal region of one dorsal blastomere at the four-cell stage. As shown in the Figure 3A, eyes are smaller on xKazrin-depleted sides (right sides). In addition, the head axis is distorted toward the Kazrin depleted side, likely resulting from smaller head structures within that half. As expected, this effect upon the size of the head does not extend to ventral depletions, as for example, those within the ventral vegetal region appeared of little consequence (Supp. Fig. S3). The specificity of xKazrin depletion was supported by the partial rescue of eye and craniofacial defects upon exogenous expression of xKazrinA (Fig. 3B,C; Table 1). Specificity was also suggested by means of use of two independent morpholinos (Kmo-1 and Kmo-S), which produced a similar range of phenotypes. Together, our results indicate that Kazrin is required in forming structures of the vertebrate head.

Likewise, xARVCF or xdelta-catenin Depletion in the Head Region Induces Eye and Craniofacial Defects

Because xARVCF- and xdelta-catenin were recently determined to bind xKazrin (Cho et al., 2010), and given that the depletion of Xp120-catenin

results in eye and craniofacial defects (Ciesiolka et al., 2004), we went on to examine the effect of depleting xARVCF or xdelta-catenin (Figs. 3A and Fig. 4, respectively). Of interest, knock-down of either catenin perturbed eye and craniofacial development, possibly reflecting the shared roles of p120-subfamily catenins and xKazrin. As exogenous expression of xdelta-catenin partially rescued the phenotypes arising from xdelta-catenin depletion (Fig. 4A,B; Table 2), the specificity of its knock-down was indicated.

xARVCF Partially Rescues Eye and Craniofacial Defects Resulting From xKazrin Depletion

To test for functional interplay between xARVCF and xKazrin during *Xenopus* eye and craniofacial development, rescue experiments using subphenotypic levels of xARVCF were performed (Fig. 3). Notably, xARVCF rescued xKazrin depletion to a similar extent as xKazrinA (Fig. 3B,C; Table 1). This suggests that xARVCF and xKazrin are functionally linked in *Xenopus* head development, consistent with their direct biochemical interaction (Cho et al., 2010).

xKazrin and xARVCF Depletion Induces Malformation of the Craniofacial Cartilage

As mentioned earlier, we observed distortion of the head axis upon xKazrin or xARVCF-catenin depletion, apparently due to a reduction in head structures on the injected side. To more clearly assay for craniofacial abnormalities following xARVCF or xKazrin depletion, we used Alcian blue staining to evaluate cartilage in the intact head (Fig. 5A), and then isolated two lower jaw cartilages (ceratohyal and ceratobranchial) for closer scrutiny (Fig. 5B). Depletion of either xARVCF or xKazrin resulted in developmental defects in cartilages that were variable in degree. Generally, the ceratohyal and ceratobranchial cartilages were smaller on the morpholino injected sides. Severely affected embryos showed underdevel-

oped ceratohyal cartilage, as shown in the ARVCF mo-1 injected sample (Fig. 5B), and some had defects in Meckel's cartilage (Fig. 5A and Suppl. Fig. S4). This suggests that Kazrin and ARVCF are used in the development of a range of craniofacial cartilages, and it is noteworthy that similar extents of abnormalities followed Kazrin versus ARVCF depletions. Comparable craniofacial cartilage malformations were observed in embryos depleted of xdelta-catenin (Supp. Fig. S5A).

xKazrin or xARVCF Depletion Appears to Result in Reduced Neural Crest Cell Induction and Migration

Because the observed defective craniofacial cartilages after Kazrin or ARVCF depletion originate from neural crest cells (NCC) (Sadaghiani and Thiebaud, 1987; Olsson and Hanken, 1996; Newman et al., 1997), it is conceivable that the xARVCF:xKazrin complex plays a role in this cell population. Indeed, whole-mount in situ hybridization using the neural crest markers *Twist* and *FoxD3* revealed that the depletion of xKazrin or xARVCF affected NCC development. After injecting Kazrin or ARVCF morpholinos, 40% and 42% of embryos respectively showed decreased expression of *twist* at stage 15–16, suggesting defective NCC establishment (Fig. 6A upper panel and Table 3). A decrease of the NCC population at this stage after depletion of Kazrin or ARVCF was also observed in whole-mount in situs of *FoxD* (Fig. 6A bottom panel, and supplemental Table S2). Of interest, it was previously reported that abnormal activation of *RhoA* inhibits NCC establishment in *Xenopus* (Broders-Bondon et al., 2007). Therefore, the xARVCF:xKazrin complex may conceivably affect NCC establishment, before migration, through known Kazrin and p120-subfamily effects upon *RhoGTPase* activity (Anastasiadis, 2007; Sevilla et al., 2008a; Cho et al., 2010). Notably, Kazrin or ARVCF depleted embryos further showed defects during the NCC migratory phase. Following Kazrin or ARVCF morpholino injections, in situ detection of *twist* at tail bud stage 20 demonstrated a lessened initial migration of all three NCC

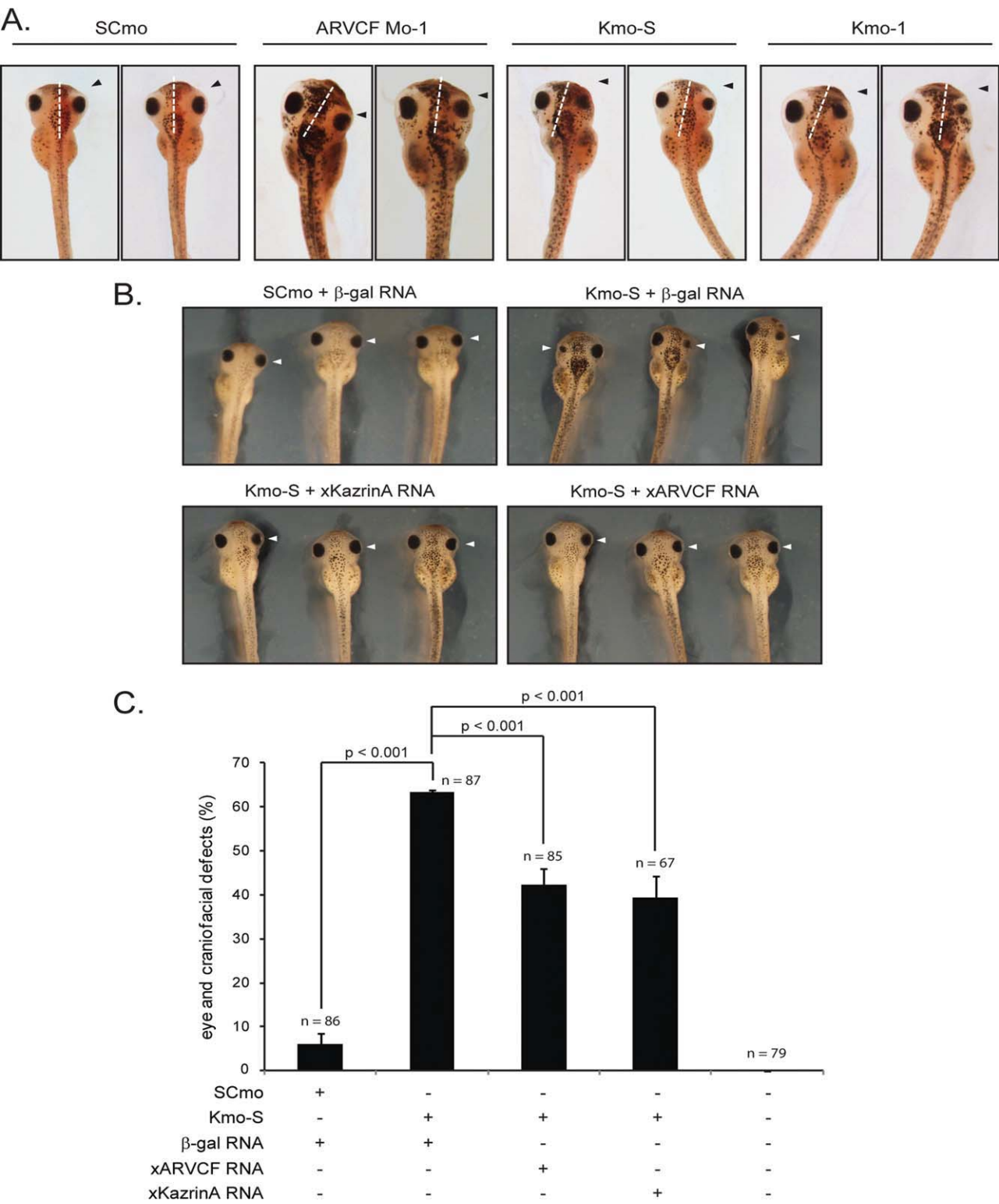


Fig. 3. Eye and craniofacial defects after xKazrin or xARVCF depletion in dorsal animal region. **A:** A total of 10 ng of xKazrin (Kmo-S) or xARVCF morpholino was micro-injected into the animal region of one dorsal blastomere at the 4-cell stage. Notably, Kmo-1 (5 ng) produced the same phenotype as Kmo-S (10 ng). As a negative control, 10 ng of standard control morpholino (SCmo) was similarly injected. Embryos were fixed with MEMFA and images recorded at tadpole stage (stage 43). White dotted lines indicate the head midline. Injected sides were stained pink because β-gal mRNA was co-injected with morpholinos and expression of β-gal detected by means of Red-gal staining. **B,C:** xARVCF as well as xKazrinA partially rescue eye & craniofacial defects resulting from xKazrin depletion. **B:** The indicated morpholino (10 ng) was co-injected with the indicated in vitro transcribed RNA (100 pg) in the animal region of one dorsal blastomere of 4-cell stage embryos. Embryo phenotypes shown are at tadpole stages (stage 41). Representative images are shown in (B), and results graphically presented in (C). Error bars reflect the standard error of the mean. Chi-Square Goodness of Fit tests were used for calculating *P* values.

TABLE 1. Rescue of Craniofacial Defects Resulting From xKazrin Depletion Via Exogenous Expression of xARVCF or xKazrinA

Injection		Number of embryos			No. of Expts.
Morpholino	RNA	Total (N)	Normal	Craniofacial defects	
10 ng SCmo	100 pg β -gal	86	78	6	3
10 ng Kmo-S	100 pg β -gal	87	31	55	3
10 ng Kmo-S	100 pg xARVCF	85	47	37	3
10 ng Kmo-S	100 pg xKazrinA	67	33	24	3
Uninjected	Uninjected	79	75	0	3

Experiments were performed as mentioned in Figure 5B.

TABLE 2. Rescue of Craniofacial Defects Resulting From x δ -Catenin Depletion Via Exogenous Expression of x δ -catenin

Injection		No. of embryos			No. of Expts.
Morpholino	RNA	Total (N)	Normal	Craniofacial defects	
10 ng SCmo	100 ng β -gal	48	47	1	2
10 ng δ -ctn Mo	100 ng β -gal	48	19	29	2
10 ng δ -ctn Mo	100 ng δ -catenin	49	33	16	2

Experiments were performed as mentioned in Figure 3B.

streams (branchial, hyoid, and mandibular) (Fig. 6B). Furthermore, the separation of the branchial NCC into the anterior (aBR) and posterior branchial streams (pBR) were not completed by stage 22 (Fig. 6C). This suggested that not only NCC establishment (induction and/ or maintenance) but also migration is affected. Appearing consistent with our findings, similar defects were previously observed following p120-catenin depletion (Ciesiolka et al., 2004). A similar decrease of NCC streams as visualized by means of snail in situ hybridization followed delta-catenin depletion (Supp. Fig. S5B). Together, our results suggest that the xARVCF:xKazrin complex contributes to both NCC establishment and migration and as a result, each has an impact upon the development of facial cartilages derived from NCC.

DISCUSSION

Our work here indicates that Kazrin is required in *Xenopus* craniofacial development, possibly by playing a role in neural crest cell (NCC) establishment and migration. Our earlier

study showed that Kazrin is a novel binding partner of p120-subfamily members such as ARVCF- and delta-catenin. In accordance with their respective biochemical association with Kazrin, we find similarly, that ARVCF- and delta-catenin are required for cranial neural crest cell establishment and migration and subsequent craniofacial development. As the depletion defects resembled those following *Xenopus* p120-catenin knock-down (Ciesiolka et al., 2004), p120-subfamily members may contribute in related manners to craniofacial formation.

An earlier study in *X. tropicalis* reported various developmental defects following Kazrin depletion, namely axis shortening, eye and head reductions, loss of epidermal integrity, and cardiac edema (Sevilla et al., 2008b). In our initial observations in *X. laevis*, likewise arising following morpholino injection at the one-cell stage, we predominantly observed abnormal dorsal structures and ectodermal shedding at neurula stages (Cho et al., 2010). One conceivable explanation for the fractional difference in observed phenotypes is that in our hands, the morpholino directed against Kazrin did not

diffuse as widely following injection, producing effects largely upon the surface ectoderm and its derivatives. To test this possibility in the current study, we depleted Kazrin in a more directed manner. We first carefully reevaluated Kazrin expression during *X. laevis* development using assays including whole-mount in situ hybridization, semi-quantitative RT-PCR and immuno-blotting. We found that Kazrin is constitutively expressed from oocyte to adult stages. Furthermore, whole-mount in situ hybridization revealed Kazrin mRNA enrichment in the neural tube, head and eye regions and pharyngeal arch. Based on this spatial expression pattern, we depleted Kazrin in the future head region by injecting Kazrin morpholinos into one dorsal blastomere (animal region) of four-cell stage embryos. To further ensure Kazrin depletion specificity, we designed a new Kazrin morpholino inhibiting normal splicing of the Kazrin pre-mRNA, and used it in parallel with a translation blocking morpholino (Kmo-1) reported in previous two studies (Sevilla et al., 2008b; Cho et al., 2010). This new morpholino gave rise to eye and head defects in *X. laevis* at high penetrance (90% of embryos effected following 20 ng Kmo-S injection), supporting Kazrin's role in these structures.

We recently reported that Kazrin binds to the p120-subfamily proteins ARVCF-, delta- and p0071-catenin (Cho et al., 2010). We additionally suggested that Kazrin enhances p190B-RhoGAP association with these catenins and the spectrin-actin cytoskeleton, leading to RhoA inhibition in junctional regions, cortical actin stabilization, and decreasing cadherin endocytosis and degradation. Congruent with their physical interaction, our present study reveals that ARVCF- or delta-catenin depletion in the future head region phenocopies Kazrin knock-down. Furthermore, the eye and head defects that followed Kazrin knock-down were partially rescued with exogenous ARVCF, supporting their functional relationship. Notably, the involvement of p120-catenin in *Xenopus* eye evagination and cranial NCC migration was previously observed (Ciesiolka et al., 2004). Similarly, independent work has shown that ARVCF depletion results in aberrant

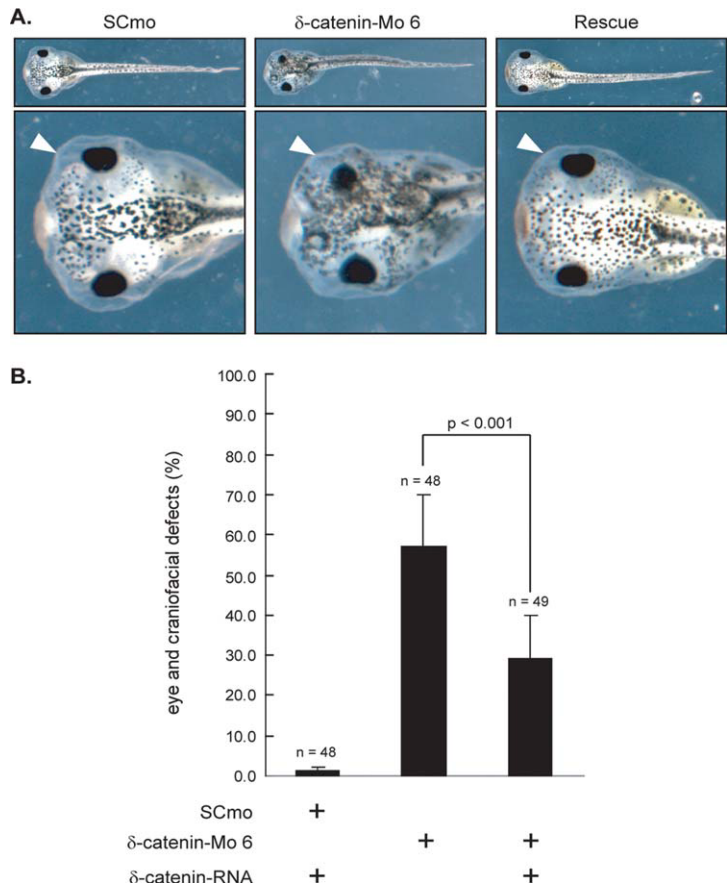


Fig. 4.

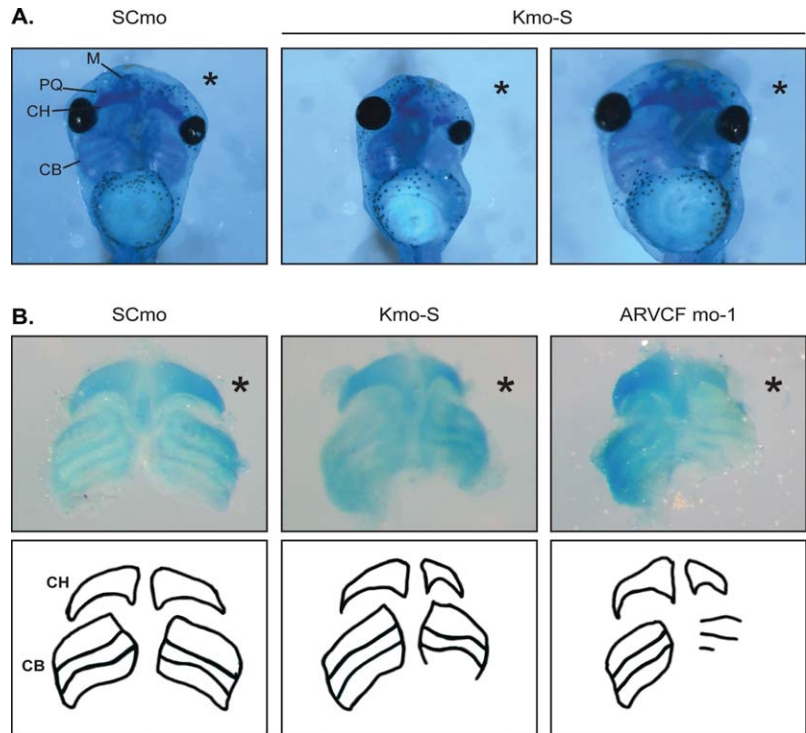


Fig. 5.

NCC migration, craniofacial and eye formation (Tran et al., 2011). In line with the biochemical association of Kazrin and p120-subfamily proteins, with the partially overlapping phenotypic outcomes for Kazrin and catenin depletion, and with our phenotypic rescues, we suggest that Kazrin, through such biochemical and functional interactions, participates in at least some p120-subfamily contributions to NCC, craniofacial, and eye development. Interestingly, in the mouse, craniofacial defects were not described following the single gene knock-out of ARVCF- or delta-catenin (Israely et al., 2004; Davis and Reynolds, 2006), with the p120-catenin null having the caveat of being an early embryonic lethal (Davis and Reynolds, 2006). When undertaken, a double deficiency of ARVCF and δ -catenin might ultimately reveal similar outcomes in the mouse as those

Fig. 4. Delta-catenin depletion in the presumptive neural ectoderm causes eye and craniofacial defects. **A:** delta-catenin-Mo 6 or SCmo (each 10 ng) was injected into one dorsal animal blastomere of eight-cell stage embryos. Exterior observation of tadpole stage embryos depleted of delta-catenin showed reduced craniofacial structures as well as eyes (middle panel), relative to SCmo injected embryos (left panel), or the uninjected side of experimental embryos. For rescues, delta-catenin RNA (titrated at 100 ng) was co-injected with the delta-catenin-Mo 6 morpholino (right panel). White arrowheads indicate the injected embryo side, while solid white lines indicate the embryo midline. **B:** Statistical analysis of phenotypes. Compared with SCmo, delta-catenin depletion resulted in significant phenotypic effects (~60% penetrance). Co-injection of a titrated dose of delta-catenin RNA leads to a partial, yet reproducible, rescue of delta-catenin knock-down. Error bar represents standard error of the mean. *P* values were obtained using Chi-Square Goodness of Fit tests.

Fig. 5. xKazrin or xARVCF depletion produced developmental defects in *Xenopus* craniofacial cartilage. **A:** Single dorsal cells (animal region) within embryos at the four-cell stage were injected with 10 ng of the indicated morpholino as noted in Figure 3. Tadpoles were fixed (stage 43), and the cartilage stained with Alcian blue dye. Asterisks (*) indicate the morpholino-injected side. Meckels (M), platoquadrate (PQ), ceratohyal (CH), and ceratobranchial (CB) cartilages are indicated. **B:** The ceratohyal and ceratobranchial cartilages were isolated from the indicated morpholino injected tadpoles, and outlined using Photoshop software (bottom panels).

TABLE 3. Defective Cranial Neural Crest Cell Development Resulting From xKazrin or xARVCF Depletion^a

Developmental stage	Morpholino	No. of embryos		
		Normal	Defective	Total (N)
Stage 15-16	SCmo	34 (85%)	6 (15%)	40
	Kmo-S	33 (60%)	22 (40%)	55
	ARVCF mo-1	14 (58%)	10 (42%)	24
Stage 18-19	SCmo	19 (73%)	7 (27%)	26
	Kmo-S	10 (34%)	19 (66%)	29
	ARVCF mo-1	16 (46%)	19 (54%)	35

^aA total of 10-15 ng of the indicated morpholino was injected into the dorsal animal region at four-cell stage embryos. Embryos were fixed at the two indicated stages, and whole-mount in situ hybridization for the Twist neural crest marker was performed. Embryos with reduced twist expression or an abnormal twist expression pattern were scored as defective.

reported for the single catenin knock-downs in *Xenopus* (Fang et al., 2004; Gu et al., 2009). The conditional knock-out of p120 in mice has been executed in tissues including epidermis, salivary gland, forebrain, and endothelial tissues (Davis and Reynolds, 2006; Elia et al., 2006; Perez-Moreno et al., 2006; Oas et al., 2010). Ultimately, a selective knock-out of p120 in NCC (Wnt1-, Pax3-, or Ht-PA-driven Cre) (Danielian et al., 1998; Li et al., 2000; Pietri et al., 2003), will be useful in evaluating its craniofacial contributions.

While our in situ marker analysis suggests that Kazrin is needed for normal amphibian NCC development, and additionally that ARVCF is required in agreement with independent work (Tran et al., 2011), Kazrin's contributions at the molecular level are not yet clear. NCC development is often described in several stages: NCC establishment (induction and maintenance), migration, and differentiation. Our current study suggests that Kazrin and ARVCF are needed for NCC establishment. Complicating matters somewhat but consistent with Kazrin's expression in the neural tube (Fig. 1D), Kazrin depletion resulted in decreased neural tube size. While requiring further study to evaluate early possible links to NCC establishment, Kazrin may thus participate in neural tube formation by affecting cell proliferation, death or differentiation. Alternatively, a previous report indicated that increased RhoA activity inhibits NCC establishment (Broders-Bondon et al., 2007).

Because Kazrin appears to act together with ARVCF (or delta-catenin) to inhibit RhoA by means of p190B-RhoGAP (Cho et al., 2010), it is conceivable that the ARVCF:Kazrin complex is primarily involved in NCC establishment by means of the modulation of RhoA activity. Kazrin may further participate in later neural crest cell differentiation, analogous to its recently reported involvement in keratinocyte differentiation (Sevilla et al., 2008a). Interestingly, in addition to its cell-cell border and cytoplasmic localization, Kazrin can enter the nucleus and associate with several transcription factors that we are now characterizing (K.C., M.S.L. & P.D.M., unpublished data). This suggests the possible involvement of Kazrin in the expression of genes important for NCC establishment and differentiation.

Finally, Kazrin and p120-subfamily proteins may modulate NCC migration by means of small-GTPase/ cytoskeletal effects. In some Kazrin- or ARVCF-depleted embryos, NCC marker staining did not appear to be altered at the NCC establishment stage, yet NCC migration was aberrant (Fig. 6C). This seems to coincide with NCC migration defects following p120 or ARVCF depletion, and with the p120 knock-down being rescued using RhoA (Ciesiolka et al., 2004) (Tran et al., 2011). Cadherins, such as cadherin-11, have also been implicated in modulating Rho-GTPase (by means of Trio-GEF), and thereby NCC migration (Kashef et al., 2009). In human cancer cells (MDA231 and

UMRC3), cadherin-11-mediated motility depends upon p120 association and RhoA inhibition (Soto et al., 2008). As would be predicted, these and other findings support small-GTPases contributions to NCC migration. Although future work is needed to understand the molecular underpinnings, possibly further involving p190B-RhoGAP (Cho et al., 2010), our work here suggests that Kazrin is involved in the context of its biochemical and functional interactions with p120-subfamily members. Overall, our study points to Kazrin's required roles in craniofacial and eye formation, and provides further support to ARVCF's and delta-catenin's essential contributions to amphibian development.

EXPERIMENTAL PROCEDURES

Xenopus Embryo Manipulations and Histological Analysis

We followed the guidelines set by the Institutional Animal Care and Use Committee of The University of Texas, M. D. Anderson Cancer Center for frog husbandry. Induction of female *Xenopus laevis*, in vitro fertilization of eggs, and embryo injections were carried out using standard methods (Sive et al., 2000). Embryos at stage 19 were fixed with Bouin fixative (Fisher), dehydrated with ethanol, embedded in paraplast (Fisher), sectioned using a microtome (American Optical Model 820), and stained with hematoxylin solution (Sigma).

xKazrin RT-PCR Primers and Morpholinos

Primers used for RT-PCR analysis of xKazrin were: F1: 5'-GAGTCGCACG ACTGCAGGTCT-3', R1 : 5'-CTATGCT GCTCATAATTCCTG-3' and R2: 5'-CTGTGGATGTCCGTGGTACAG-3'. The sequence of the Kazrin splice junction blocking morpholino (Kazrin Mo-S) is 5'-AAACCATTTTGCCTC ACCTTTCT-3'. A standard control morpholino (Control-Mo) from Gene Tools LLC was used as a negative control (5'-CCTCTTACCTCAGTTACAAT TTATA-3').

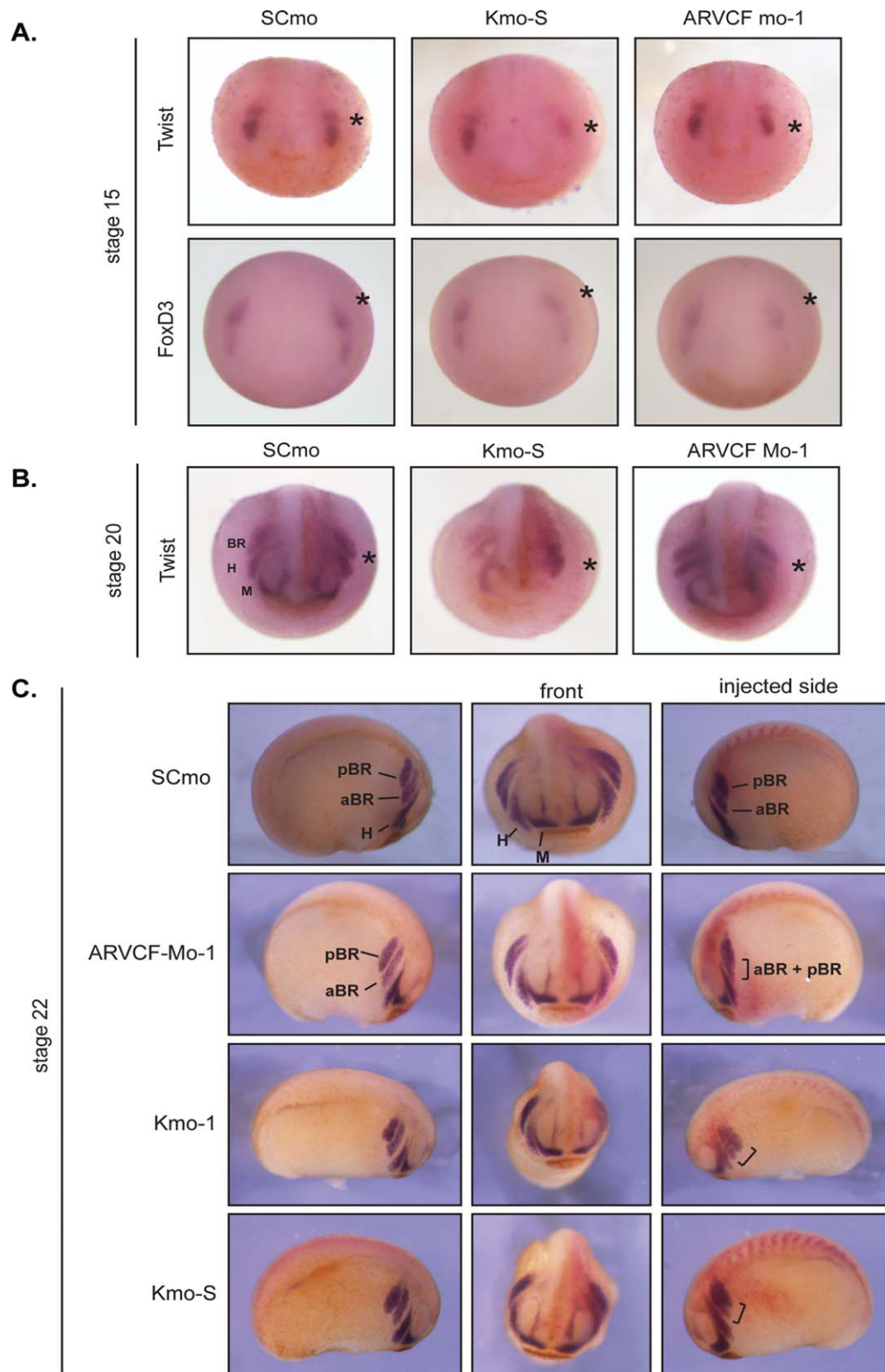


Fig. 6. xKazrin or xARVCF depletion perturbs the expression of neural crest cell markers. **A:** The indicated morpholinos (20 ng) were injected into the animal region of one dorsal blastomere (animal region) of four-cell embryos. At early neurula stages (stage 15), embryos were fixed and neural crest cells visualized using whole-mount in situ hybridization for two neural crest markers: Twist and FoxD3. **B,C:** Embryos were fixed at early tail bud stages, stages 20 and 22 (respectively B and C) and whole-mount in situ hybridization for twist was performed. Unseparated branchial neural crest cell streams are indicated by brackets. Asterisks (*) indicate the injected side. Br, Branchial neural crest cells; aBR, anterior branchial neural crest cells; pBR, posterior branchial neural crest cells; H, Hyoid neural crest cells; M, Mandibular neural crest cells.

Embryo / Adult Tissue Lysates and Immuno-Blotting for Endogenous *Xenopus* Proteins

Xenopus embryos at the indicated stages were collected and lysed in TX100 Lysis Buffer. Protein extracts were subjected to immuno-blotting using IgG-purified anti-xKazrin antibody, and anti-actin antibody (Sigma, A-2066). Adult *Xenopus* tissue extracts were prepared by sacrificing one frog in accordance with an approved protocol followed by surgical isolation of the indicated tissues. Samples were homogenized in modified RIPA buffer (50 mM Tris-HCl pH 7.4, 1% NP-40, 0.25% Na-deoxycholate, 150 mM NaCl, 1 mM ethylenediaminetetraacetic acid [EDTA], 1 mM PMSF, 1 mM Na₃VO₄, 1 mM NaF, and 1 µg/ml each of Aprotinin, leupeptin, and pepstatin) using a dounce homogenizer and centrifuged at 15,000 rpm for 30 min. Cleared supernatants (35 µg) were analyzed by immuno-blotting using the IgG-purified anti-xKazrin antibody, and a polyclonal anti-actin antibody (loading control).

The anti-xC-cadherin and anti-xARVCF antibodies were previously described (Fang et al., 2004).

Alcian Blue Staining

For cartilage staining, embryos were fixed in 95% ethanol overnight and incubated overnight in Alcian blue solution (Sigma A3157; 150 mg of Alcian blue in 800 ml of 95% ethanol and 200 ml of acetic acid). Stained embryos were washed with 95% ethanol for 4–5 hr. Embryos were soaked in 2% KOH for 1–2 hr(s) until the skin became soft. After removal of the skin, the cartilage was visualized.

Whole-Mount In Situ Hybridization

Whole-mount in situ hybridization was performed according to a previously reported protocol (Sive et al., 2000). In brief, embryos were fixed in MEMFA fixative, dehydrated in methanol, re-hydrated with serially diluted methanol, re-fixed with 4% paraformaldehyde, prehybridized in hybridization buffer (50% formamide, 5× standard saline citrate [SSC], 1 mg/

ml yeast RNA, 100 µg/ml heparin, 1× Denhart's solution, 0.1% Tween 20, 0.1% CHAPS and 10 mM EDTA) at 60°C for 6 hr, and hybridized with digoxigenin labeled RNA probes at 60°C overnight. After washing with SSC solution, embryos were incubated in blocking solution (2% blocking reagent in maleic acid buffer) at room temperature for 1 hr and then incubated with anti-digoxigenin antibody conjugated to alkaline phosphatase overnight at 4°C. Targeted RNAs were visualized using a NBT/BCIP (nitroblue tetrazolium/5-bromo-4-chloro-3-indolyl phosphate) substrate color reaction for alkaline phosphatase, and embryos were re-fixed in Bouin fixative overnight. Embryos were washed with 70% ethanol until the Bouin fixative's yellow tint was removed, followed by bleaching (0.5× SSC, 5% formamide, and 1.2% peroxide), and observation under a stereomicroscope.

Statistical Analysis

For each analysis, we divided the phenotypes into two categories, eye and craniofacial defects versus other, that included several less consistent or unrelated defects such as in gastrulation. To account for differences in the total numbers of control versus experimental embryos within groups, the data were converted to percentages and graphs were produced based on the average percentages of repeated experiments. To analyze the significance of our phenotypes and given our countable numeric data, we used the chi-square goodness of fit test. To obtain *P*-values, we hypothesized that the two groups are statistically identical (null hypothesis), and analyzed the data using the chi-square test (CHITEST) within the Microsoft Excel software program.

ACKNOWLEDGMENTS

We thank K. Vleminckx (U. Gent) for sharing his knowledge and reagents. We also thank S. Sokol for kindly provisioning the FoxD3 in situ probe. For statistical analysis, we consulted and appreciated the assistance of T. Choi (Korea University). P.D.M. was funded by the National Institutes of Health, a Texas ARP Grant, and an Institutional Research Grant. K.C. was supported in part by a Hearst Foundation Stu-

dent Research & Education Award. DNA sequencing and other core facilities were supported by a University of Texas MD Anderson Cancer Center NCI Core Grant.

REFERENCES

- Anastasiadis PZ. 2007. p120-ctn: A nexus for contextual signaling via Rho GTPases. *Biochim Biophys Acta* 1773:34–46.
- Anastasiadis PZ, Moon SY, Thoreson MA, Mariner DJ, Crawford HC, Zheng Y, Reynolds AB. 2000. Inhibition of RhoA by p120 catenin. *Nat Cell Biol* 2: 637–644.
- Bennett V, Healy J. 2009. Membrane domains based on Ankyrin and Spectrin associated with cell-cell interactions. *Cold Spring Harbor Perspect Biol* 1: a003012.
- Broders-Bondon F, Chesneau A, Romero-Oliva F, Mazabraud A, Mayor R, Thiery JP. 2007. Regulation of XSnail2 expression by Rho GTPases. *Dev Dyn* 236: 2555–2566.
- Cho K, Vaught TG, Ji H, Gu D, Papasakelariou-Yared C, Horstmann N, Jennings JM, Lee M, Sevilla LM, Kloc M, Reynolds AB, Watt FM, Brennan RG, Kowalczyk AP, McCreas PD. 2010. *Xenopus* Kazrin interacts with ARVCF-catenin, spectrin and p190B RhoGAP, and modulates RhoA activity and epithelial integrity. *J Cell Sci* 123:4128–4144.
- Ciesiolka M, Delvaeye M, Van Imschoot G, Verschuere V, McCreas P, van Roy F, Vleminckx K. 2004. p120 catenin is required for morphogenetic movements involved in the formation of the eyes and the craniofacial skeleton in *Xenopus*. *J Cell Sci* 117:4325–4339.
- Danielian PS, Muccino D, Rowitch DH, Michael SK, McMahon AP. 1998. Modification of gene activity in mouse embryos in utero by a tamoxifen-inducible form of Cre recombinase. *Curr Biol* 8:1323–1326.
- Davis MA, Reynolds AB. 2006. Blocked acinar development, E-cadherin reduction, and intraepithelial neoplasia upon ablation of p120-catenin in the mouse salivary gland. *Dev Cell* 10:21–31.
- Davis MA, Ireton RC, Reynolds AB. 2003. A core function for p120-catenin in cadherin turnover. *J Cell Biol* 163:525–534.
- Elia LP, Yamamoto M, Zang K, Reichardt LF. 2006. p120 catenin regulates dendritic spine and synapse development through Rho-family GTPases and cadherins. *Neuron* 51:43–56.
- Fang X, Ji H, Kim SW, Park JI, Vaught TG, Anastasiadis PZ, Ciesiolka M, McCreas PD. 2004. Vertebrate development requires ARVCF and p120 catenins and their interplay with RhoA and Rac. *J Cell Biol* 165:87–98.
- Groot KR, Sevilla LM, Nishi K, DiColandrea T, Watt FM. 2004. Kazrin, a novel periplakin-interacting protein associated with desmosomes and the keratinocyte plasma membrane. *J Cell Biol* 166:653–659.

- Grosheva I, Shtutman M, Elbaum M, Bershadsky AD. 2001. p120 catenin affects cell motility via modulation of activity of Rho-family GTPases: a link between cell-cell contact formation and regulation of cell locomotion. *J Cell Sci* 114: 695–707.
- Gu D, Sater AK, Ji H, Cho K, Clark M, Stratton SA, Barton MC, Lu Q, McCreas PD. 2009. *Xenopus* (δ)-catenin is essential in early embryogenesis and is functionally linked to cadherins and small GTPases. *J Cell Sci* 122:4049–4061.
- Huber AH, Nelson WJ, Weis WI. 1997. Three-dimensional structure of the armadillo repeat region of beta-catenin. *Cell* 90:871–882.
- Iretton RC, Davis MA, van Hengel J, Mariner DJ, Barnes K, Thoreson MA, Anastasiadis PZ, Matrisian L, Bundy LM, Sealy L, Gilbert B, van Roy F, Reynolds AB. 2002. A novel role for p120 catenin in E-cadherin function. *J Cell Biol* 159: 465–476.
- Israely I, Costa RM, Xie CW, Silva AJ, Kosik KS, Liu X. 2004. Deletion of the neuron-specific protein delta-catenin leads to severe cognitive and synaptic dysfunction. *Curr Biol* 14:1657–1663.
- Kashef J, Kohler A, Kuriyama S, Alfandari D, Mayor R, Wedlich D. 2009. Cadherin-11 regulates protrusive activity in *Xenopus* cranial neural crest cells upstream of Trio and the small GTPases. *Genes Dev* 23:1393–1398.
- Kikuno R, Nagase T, Ishikawa K, Hiro-sawa M, Miyajima N, Tanaka A, Kotani H, Nomura N, Ohara O. 1999. Prediction of the coding sequences of unidentified human genes. XIV. The complete sequences of 100 new cDNA clones from brain which code for large proteins in vitro. *DNA Res* 6:197–205.
- Li J, Chen F, Epstein JA. 2000. Neural crest expression of Cre recombinase directed by the proximal Pax3 promoter in transgenic mice. *Genesis* 26:162–164.
- Mariner DJ, Wang J, Reynolds AB. 2000. ARVCF localizes to the nucleus and adherens junction and is mutually exclusive with p120(ctn) in E-cadherin complexes. *J Cell Sci* 113(pt 8): 1481–1490.
- McCreas PD, Gu D. 2010. The catenin family at a glance. *J Cell Sci* 123:637–642.
- Nachat R, Cicolat S, Sevilla LM, Chhatr-wala M, Groot KR, Watt FM. 2009. KazrinE is a desmosome-associated liprin that colocalises with acetylated microtubules. *J Cell Sci* 122:4035–4041.
- Newman CS, Grow MW, Cleaver O, Chia F, Krieg P. 1997. Xbap, a vertebrate gene related to bagpipe, is expressed in developing craniofacial structures and in anterior gut muscle. *Dev Biol* 181: 223–233.
- Noren NK, Liu BP, Burrige K, Kreft B. 2000. p120 catenin regulates the actin cytoskeleton via Rho family GTPases. *J Cell Biol* 150:567–580.
- Oas RG, Xiao K, Summers S, Wittich KB, Chiasson CM, Martin WD, Grossniklaus HE, Vincent PA, Reynolds AB, Kowalczyk AP. 2010. p120-Catenin is required for mouse vascular development. *Circ Res* 106:941–951.
- Ohkubo T, Ozawa M. 1999. p120(ctn) binds to the membrane-proximal region of the E-cadherin cytoplasmic domain and is involved in modulation of adhesion activity. *J Biol Chem* 274:21409–21415.
- Olsson L, Hanken J. 1996. Cranial neural-crest migration and chondrogenic fate in the oriental fire-bellied toad *Bombina orientalis*: defining the ancestral pattern of head development in anuran amphibians. *J Morphol* 229:105–120.
- Perez-Moreno M, Davis MA, Wong E, Pasolli HA, Reynolds AB, Fuchs E. 2006. p120-catenin mediates inflammatory responses in the skin. *Cell* 124:631–644.
- Pietri T, Eder O, Blanche M, Thiery JP, Dufour S. 2003. The human tissue plasminogen activator-Cre mouse: a new tool for targeting specifically neural crest cells and their derivatives in vivo. *Dev Biol* 259:176–187.
- Sadaghiani B, Thiebaud CH. 1987. Neural crest development in the *Xenopus laevis* embryo, studied by interspecific transplantation and scanning electron microscopy. *Dev Biol* 124:91–110.
- Schmelzl B, Geli MI. 2002. An efficient genetic screen in mammalian cultured cells. *EMBO Rep* 3:682–687.
- Sevilla LM, Nacht R, Groot KR, Watt FM. 2008a. Kazrin regulates keratinocyte cytoskeletal networks, intercellular junctions and differentiation. *J Cell Sci* 121:3561–3569.
- Sevilla LM, Rana AA, Watt FM, Smith JC. 2008b. KazrinA is required for axial elongation and epidermal integrity in *Xenopus tropicalis*. *Dev Dyn* 237:1718–1725.
- Singh G, Lykke-Andersen J. 2003. New insights into the formation of active nonsense-mediated decay complexes. *Trends Biochem Sci* 28:464–466.
- Sive HL, Gaignier RM, Harland RM. 2000. Early development of *Xenopus laevis*: a laboratory manual. Cold Spring Harbor Laboratory Press. p 249–297.
- Soto E, Yanagisawa M, Marlow LA, Copland JA, Perez EA, Anastasiadis PZ. 2008. p120 catenin induces opposing effects on tumor cell growth depending on E-cadherin expression. *J Cell Biol* 183:737–749.
- Thoreson MA, Anastasiadis PZ, Daniel JM, Iretton RC, Wheelock MJ, Johnson KR, Hummingbird DK, Reynolds AB. 2000. Selective uncoupling of p120(ctn) from E-cadherin disrupts strong adhesion. *J Cell Biol* 148:189–202.
- Tran HT, Delvaeye M, Verschuere V, Descamps E, Crabbe E, Van Hoorebeke L, McCreas P, Adriaens D, Van Roy F, Vleminckx K. 2011. ARVCF depletion cooperates with Tbx1 deficiency in the development of 22q11.2DS-like phenotypes in *Xenopus*. *Dev Dyn* 240: 2680–2687.
- Wang Q, Liu M, Li X, Chen L, Tang H. 2009. Kazrin F is involved in apoptosis and interacts with BAX and ARC. *Acta Biochim Biophys Sin (Shanghai)* 41: 763–772.
- Xiao K, Allison DF, Buckley KM, Kottke MD, Vincent PA, Faundez V, Kowalczyk AP. 2003. Cellular levels of p120 catenin function as a set point for cadherin expression levels in microvascular endothelial cells. *J Cell Biol* 163:535–545.
- Xiao K, Garner J, Buckley KM, Vincent PA, Chiasson CM, Dejana E, Faundez V, Kowalczyk AP. 2005. p120-Catenin regulates clathrin-dependent endocytosis of VE-cadherin. *Mol Biol Cell* 16: 5141–5151.
- Yap AS, Niessen CM, Gumbiner BM. 1998. The juxtamembrane region of the cadherin cytoplasmic tail supports lateral clustering, adhesive strengthening, and interaction with p120ctn. *J Cell Biol* 141:779–789.